STUDY OF THE THREE-PHASE FLUID FLOW MECHANISM IN LOW PERMEABILITY AND HIGH GOR RESERVOIRS

JIA Ninghong[1], LV Weifeng[1*], LIU Qingjie[1], QIN Jianhua[2], XU Changfu[2], Danyong LI[3], LENG Zhenpeng[1]

1. State Key Laboratory of Enhanced Oil Recovery, Research Institute of Petroleum Exploration and Development, Beijing, China; 2. Research Institute of Exploration And Development of Xinjiang Oilfield Company, CNPC, Karamay, China; 3, iRock Technologies, Beijing, China

This paper was prepared for presentation at the International Symposium of the Society of Core Analysts held in Snowmass, Colorado, USA, 21-26 August 2016

ABSTRACT

Multiphase flow induced by solution gas evolution impacts water flooding performance, such as drastically decline of oil and liquid production, which raises the necessity to take into account the gas evolution effect when designing oilfield development plan and optimizing oilfield development model. In this work a three-phase flow experiment was conducted to simulate water flooding process in a core sample from one low permeability reservoir with high GOR located in northwestern China and the impact of solution gas evolution was studied quantitatively. By imaging the flooding process in a core sample with an X-ray CT facility and recording the variance profile of gas saturations on multiple locations of the core sample was observed. Also, relative permeability of oil phase is reduced by 27.5% from that of two-phase (oil/water) flow where solution gas evolution effect is omitted. On the other hand, reduction of relative permeability of water phase is only 1.4%, indicating that water phase flow is less impacted by solution gas evolution, assuming a water-wet reservoir where water-phase has little direct contact with gas-phase.

INTRODUCTION

Water flooding is often approached as an effective way for oil production in low permeability reservoirs featuring low formation energy. However, rapid dissipation of the injected energy due to high flow resistance of low permeability reservoirs makes it difficult to supplement adequate energy in time to support the formation pressure. Solution gas tends to come out of crude oil as the formation pressure drops below the saturation pressure point, which is a prevalent occurrence near wellbore area, particularly for low permeability reservoirs with high GOR (Gas/oil ratio). [1-2]

Higher saturation pressure would be beneficial in solution gas drive since it permits higher drawdown pressure. The effect of increased GOR at a constant saturation pressure due to compositional effects is not obvious. Increased GOR would give lower live oil viscosity and increased gas flow. [3]

In all solution gas drive reservoirs, gas is released from solution as formation pressure declines, initially in the form of tiny bubbles within individual pore bodies. As formation pressure declines further, the tiny bubbles expand to occupy connected pores. Eventually the bubbles expand large enough due to very low pressure and merge each other into a continuous gas phase. [4]

Although the understanding of solution gas drive has been intensively studied in recent years, the flow mechanism of solution gas drive in porous medium still remains unclear enough [5-6], although microscopic flow behavior can be observed in micro-models by various approaches. There still exists certain representative issue of microscopic pore spaces to realistic pore spaces, as well as different temperature and pressure between underground formation condition and at room conditions. This study uses core sample of realistic length scale at reservoir pressure and temperature and applies CT scanning process to identify the place where solution gas appears and to observe the solution gas evolution.

EXPERIMENTAL

Core Samples and Fluids

Two core plugs, 5 inches in length and 1 inch in diameter, were drilled from a block of conglomerate using liquid nitrogen as coolant, dried in an oven at 110°C for 3 days and cooled in a desiccator for 2 days. The plugs (Sample XJ1 and Sample XJ2) were then imaged by X-ray CT facility to investigate their homogeneity and comparability. The three-dimensional images of the samples demonstrated that they were heterogeneous. Air permeabilities of Samples XJ1 and XJ2 were 1.6mD and 1.4mD, respectively, and they have close average CT number which shows Sample XJ1 and Sample XJ1 can be used as parallel reference samples. Figure 1 shows the distribution of porosity along the length of the core for both sample XJ1 and sample XJ2 and the petrophysical parameters are shown in Table 1. The test live oil was made by dissolving CO2 and CH4 into crude oil with mole ratio 19:97, which has a solution gas oil ratio (GOR) of 179.0m3/m3, viscosity of 26.12mPa·s, density of 0.7165 g/cm3, bubble point pressure (BBP) of 10.07MPa at reservoir conditions of 53.7°C.

Experimental Set-up and Conditions

The scheme of the experimental set-up is illustrated in Figure 2. A medical CT scanner manufactured by GE was used as a base platform where a set of core flooding experimental equipment was attached to realize the function of simultaneous scanning and flooding. The core samples and the fluids were scanned at low energy (100kV) and high energy (140kV) respectively by changing the volt of the X-ray source, and the filament current was fixed at 150mA. Helical mode was adopted to reduce the scanning time. CT images were processed by CT image analysis software (CTIAS 2.0, developed by RIPED). Two sets of QUIZIX pumps were employed to control the injection of water and oil. A set of ISCO pumps was used to control the back pressure. Image slices from the scanning were taken as platforms for the three-phase saturation calculations [7].

PROCEDURES

A workflow of simulating the evolved gas-driving flooding experiment by displacing the crude oil containing solution gas with injected brine is designed and carried out on the proposed experimental configuration. This workflow is a modification and extension of our previous traditional water flooding experiment on core samples with the aid of Dual-energy X-ray CT scanning and imaging processing. The procedures of the workflow are proposed as following:

1. A core sample is vacuumed within the core holder with a confining pressure of 20MPa. The same gas as the solution gas in oil is injected into the vacuumed core sample till full saturation. Then, X-ray CT imaging is performed and the image slices obtained are taken as ‘dry model’.
2. The gas saturated core sample is re-vacuumed and white oil is injected until it reaches full saturation. Then, the live crude oil *is* injected into the core sample to displace the white oil. The reason that live crude oil displaces white oil instead of being directly injected into the vacuumed pore space is to avoid that the unexpected gas is coming out due to extremely low pressure in the vacuumed pore space. X-ray CT images obtained by scanning the core sample with fully saturated crude oil are taken as ‘oil-wet model’.
3. After core sample with saturated crude oil is scanned by X-ray CT, the sample is then cleaned by alternately injecting petroleum ether and air into the sample until it is believed that no petroleum ether remains within the core sample.
4. The vacuumed core sample is once again saturated by injecting brine and the X-ray CT image slices obtained are taken as ‘water-wet model’.
5. A pressure-controlled live crude oil injection is carried out on the brine saturated core sample, with initial pressure starting from 12MPa. The pressure is incremented until no water is produced at the outlet of the sample. X-ray CT image slices obtained at this stage are considered to be the initial reservoir condition prior to production, hence labelled as ‘initial-model’
6. Production stage is simulated by injecting brine into the crude-oil-saturated sample while the pressure and flow rate is measured at the outlet end. The injection is controlled to maintain a constant flow rate during the whole procedure and injecting pressure is gradually incremented till the maximum pressure of 17MPa. Various injecting stages are scanned by X-ray CT and are labelled as ‘intermedia models’. This procedure stops as no more oil and gas are produced at the outlet.

RESULTS AND DISCUSSION

Gas saturation of sample XJ1 calculated from the CT image slices shows in Figure 3 that no gas coming out in the first half section of the sample. As back pressure declines from 12MPa to 8MPa, gas begins to come out near the outlet end and the region where dissolved gas can be detected occupies the second half section of the core sample. It is obvious that gas saturation increases as pressure goes down, which is consistent with the reservoir observation that more gas evolves from the solution as pressure declines.

With permeability and porosity close to sample XJ1, sample XJ2 is taken as a parallel reference sample and performed with the same workflow except that on XJ2 the back pressure declines to 4MPa, instead of 8MPa on XJ1. Figure 4 compares the gas production of the two samples with different declining pressures. It can be observed that gas evolution in XJ2 occupies larger section of a core sample than that in XJ1. Further, the effect of higher declined pressure leads to higher gas production from XJ2 (16%) than that of XJ1 (10%).

Overlapping relative permeability curves of XJ1 and XJ2 and comparing them with regular two-phase relative permeability curves can obviously shows in Figure 5 the effect of higher declined pressure at the outlet end. The reduction of the oil-phase relative permeability by the impact of gas evolution is proportional to the magnitude of the declined pressure. Relative permeability of oil phase is reduced by 27.5% on XJ2 from that of two-phase (oil/water) flow. On the other hand, reduction of relative permeability of water phase is only 1.4%, indicating that water phase flow is less impacted by solution gas evolution, assuming a water-wet reservoir where water-phase has little direct contact with gas-phase.

As mentioned already, Three-phase saturations in this study were measured in-situ using computed tomography. To calculate three phase saturations, the cores were scanned at two different energy levels during the experiments and three phase relative permeability was obtained by assuming that relative permeability of each phase was a function of its own saturation. Combining with the measured gas production at the outlet end, the flow ability of oil phase in the core sample is significantly depressed by large volume of gas evolved into the pore space, which is consistent with the microscopic explanation of 2-phase flowing mechanism in porous media. On the other hand, the dissolved gas has little impact on the relative permeability of water phase through the whole production stage except on the residual water saturation.

CONCLUSION

A modified flooding experiment, combined with X-ray CT scanning, is proposed to study the characteristic of gas evolution occurrence within the pore space during production stage. It can be concluded that three-phase flowing, which implies the gas coming out occurs mainly near the outlet end of a flooded core sample.

Comparison between 2-phase (oil/water) flow and 3-phase relative permeability shows that gas evolved will depress the previous 2-phase oil-water flowing channels, hence leads to a significant reduction of oil-phase production by about 20%, while water-phase production remains much less impacted, which is consistent with the theoretical model of 3-phase flowing in channels.

ACKNOWLEDGEMENTS

We gratefully acknowledge financial support from PetroChina Research Project (2014A-1003) and Research Institute of Exploration and Development, Xinjiang Oil field Company.

REFERENCES

1. TANG, G.Q., SAHNI, A., GADELLE, F., KUMAR, M., and KOVSCEK, A.R., Heavy-Oil Solution Gas Drive in Consolidated and Unconsolidated Rock, *SPE 87226, International Thermal Operations and Heavy-Oil Symposium and Western Regional Meeting, Bakersfield, California, 2004.*
2. MAINI, B.B. Effect of Depletion Rate on Performance of Solution Gas Drive in Heavy Oil System,*SPE 81114 presented at the Latin American and Caribbean Petroleum Engineering Conference, Port-of-Spain, Trinidad and Tobago, April 27-300, 2003.*
3. Baibakov, N. K. and Garushev, A. R., Thermal Methods of Petroleum Production, *Developments in Petroleum Science* 25, *Translated by W. J. Cieslewicz, Elsevier Science, Amsterdam, pp. 6–21, 1989.*
4. SHENG, J.J., MAINI, B.B., HAYES, R.E. and TORTIKE, W.S. Critical Review of Foamy Oil Flow, *Transport in Porous Media, Vol.35, p.157-187,1999.*
5. AKIN, S., and KOVSCEK, A.R., Computed Tomography in Petroleum Research. *Applications of X-ray Computed Tomography in the Geosciences, Geological Society of London, Special Publications, 215, 23-38, 2003.*
6. SMITH, G.E., Fluid Flow and Sand Production in Heavy-Oil Reservoirs Under Solution-Gas Drive, *SPE, P169-180, May, 1988.*
7. Coles M. E., Muegge E. L., et al. “The Use of Attenuation Standards for CT Scanning,” *SCA 1995-13*, (1995).

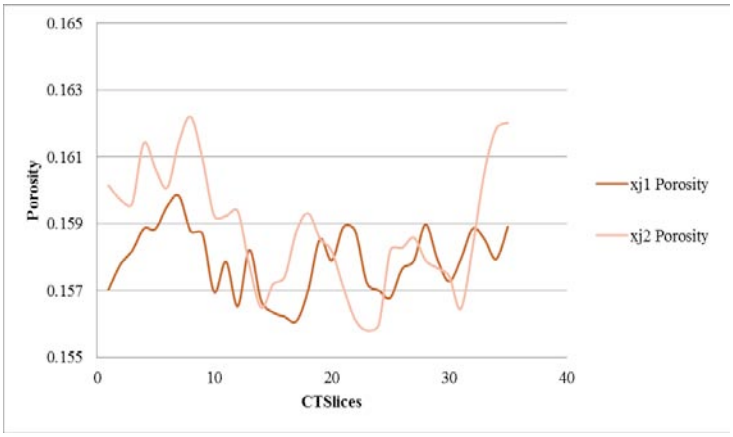

Figure 1. Slice-averaged porosity distribution along the length of the core samples determined using X-ray imaging.

Table 1. Petrophysical Parameters of Core Samples

Sample No.	Porosity,%	K_{air},10^{-3} μm^2	CT number
XJ1	15.7	1.6	2053
XJ2	16.1	1.4	2098

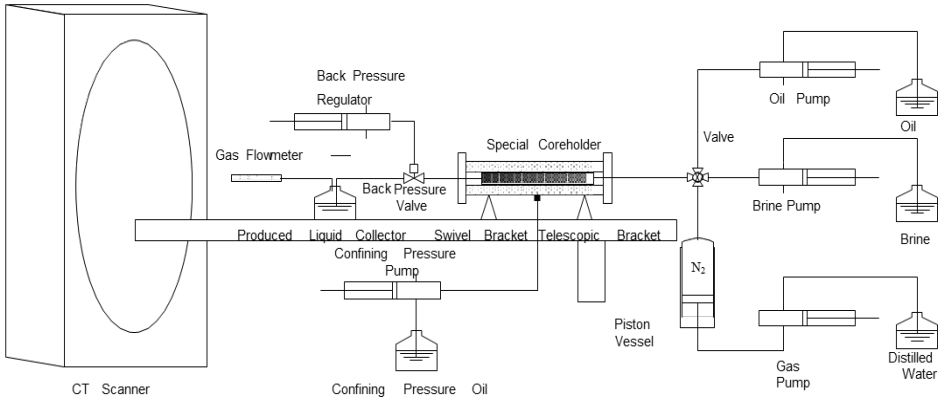

Figure 2. Experimental Schematic

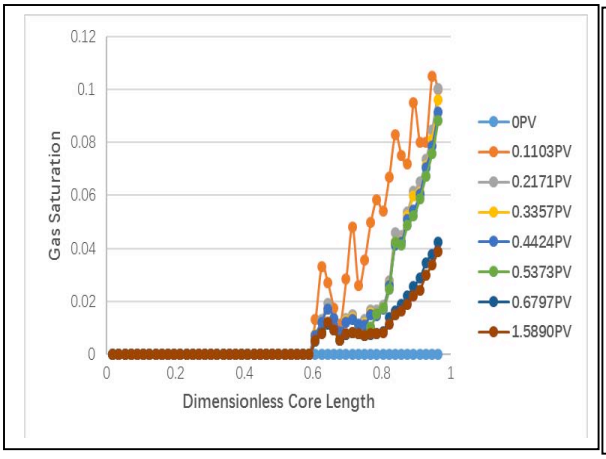

Figure 3. Gas Saturation distribution changes along the length of the sample XJ1 when back pressure declines from 12MPa to 8MPa

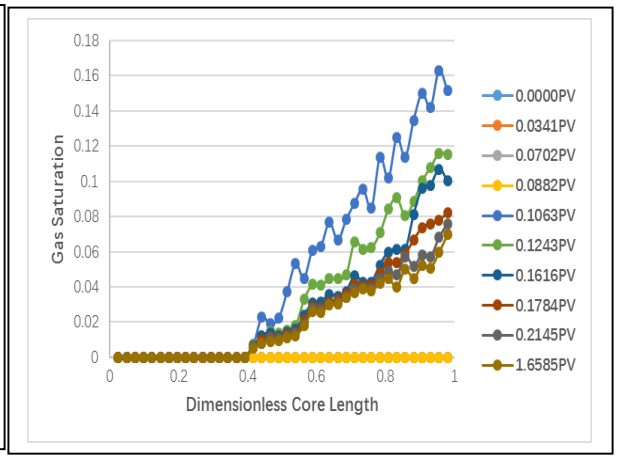

Figure 4. Gas Saturation distribution changes along the length of the sample XJ2 when back pressure declines from 12MPa to 4MPa

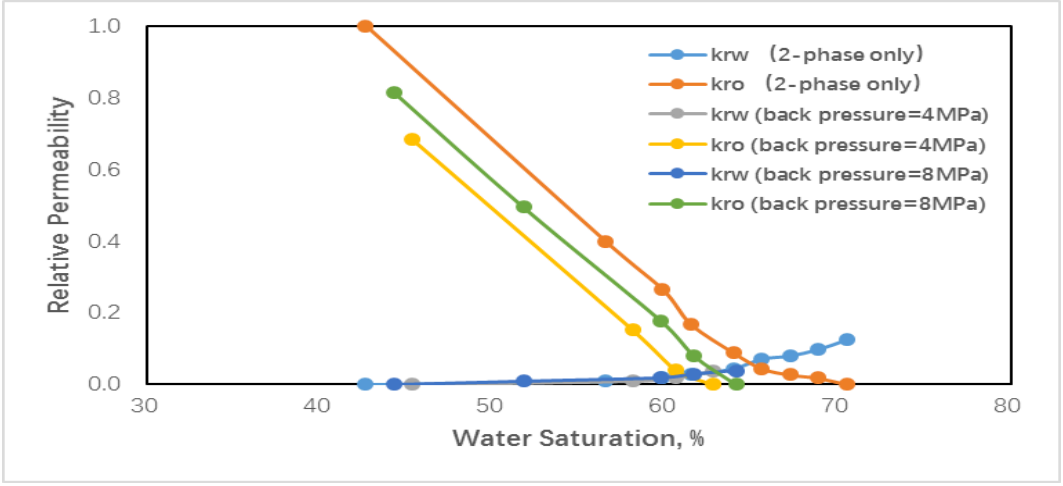

Figure 5. Comparison of relative permeability for 2-phase flow and 3-phase flow